

## SUPPLEMENTAL METHODS

### *Mice:*

The profound gender bias for the IgA phenotype in BAFF-Tg mice most likely results from sexual dimorphism in expression in the kidneys of the  $\alpha$ 1-antitrypsin (AAT) driven transgene. Transcriptional profiling of the male and female kidneys showed a 10 to 20 fold increase in the males of three of the endogenous AAT isoforms (data not shown). Tg insertion at unusual sites in the genome may be a factor, however, extreme gender bias in another AAT driven transgene was reported previously (1). Another line of TWEAK transgenic mice generated in our colony with the same promoter construct did not show a gender bias (data not shown). However, in contrast to these BAFF-Tg mice, transgenic TWEAK expression in these mice was dominated by liver expression.

Regarding the BAFF-Tg x IgA<sup>-/-</sup> cross, there were two areas of complexity in this experiment. First, IgA<sup>-/-</sup> mice probably have a different spectrum of commensal bacteria because the loss of AID expression and hence loss of IgA was reported to result in excess segmented filamentous bacteria in the gut (2). An altered flora could have influenced the immune system as evidenced by the critical role of segmented filamentous bacteria in the generation of Th17 cells and the development of EAE disease (3-5). Second, in the mice on an IgA<sup>-/-</sup> background, the Igh locus is 129 derived. The 129 strain has been typically associated with enhanced autoimmunity and, moreover, Igh<sup>a</sup> mice make IgG2<sub>a</sub> antibodies (6). These mice were then compared to mice with a C57BL/6 Igh<sup>b</sup> locus with IgG2<sub>c</sub> expression and no IgG2<sub>a</sub>. We doubt that this had an impact because IgG2<sub>a</sub> and IgG2<sub>c</sub> bind similarly to Fc $\gamma$ R.

### *Serological Analyses*

Reactivity to DNA was also assessed using a Crithidia assay. Crithidia anti-nDNA test kit (Antibodies Incorporated) were stained with serum (1:10 dilution) followed by FITC- conjugated goat anti-IgG or IgM (Southern Biotech) or biotinylated rat anti-IgA (Pharmingen) and Streptavidin conjugated Rhodamine Red-X. DAPI stain (blue) was used to visualize total DNA.

### *Western Blot*

Assessment of IgA and secretory chain: Fractions from sizing column were run on a 4-20% SDS-PAGE gel under non-reducing conditions and transferred to membrane. Separate blots were assessed for murine IgA (anti-mouse IgA-HRP) or secretory chain (rabbit anti-human secretory component (Dako) with sufficient crossover onto mouse protein followed by an Fab2 goat anti-rabbit Ig-HRP). Human colostrum IgA (Sigma) and mouse fecal extracts served as positive controls.

### *Flow Cytometry*

Lamina propria and Peyer's patch samples were isolated essentially as described in Current Protocols in Immunology. Briefly, small intestines were removed between the stomach and the cecum and then flushed with cold HBSS + 2% FBS. Intestines were then cleaned of fat and mesentery using forceps. Peyer's patches were then removed by cutting them from the surrounding tissue and then

set aside. Remaining intestines were then cut end-to-end and then into small pieces. Pieces were washed several times in cold HBSS + 2% FBS, then shaken in HBSS + 10% FBS + 5mM EDTA for 20 minutes at room temperature. Supernatant was removed and replaced with fresh EDTA solution for multiple washes and shaking cycles until the supernatant was clean. Pieces were then washed three times in cold HBSS to remove EDTA. Finally, intestinal pieces or Peyer's patches were transferred to fresh 50 ml tubes to be digested in 37°C RPMI + 10% FBS + 1 mg/ml collagenase IV (Sigma) and 200 µg/ml DNase I (Roche). After 1 hour of digestion, tubes were vortexed to disperse digested tissue. Samples were then filtered through 40 µm filters and cells collected for staining.

Bone marrow was flushed from femurs. For spleen and lymph nodes, tissues were disrupted with frosted glass slides and red blood cell lysis was performed. In all cases, single cell suspensions were first blocked with an Fc receptor blocking monoclonal antibody (2.4G2), and then cells were stained with the following mouse-specific antibodies: anti-IgA-FITC (Southern Biotech), anti-B220-APC, anti-IgM-PerCP-Cy5.5, anti-CD19-PerCP-Cy5.5, anti-CD11b-PE-Cy7, anti-CD23-biotin 7G6-FITC (all from eBioscience and anti-CD138-PE (BD Pharmingen). Samples were acquired on a BD FACS Calibur and analysed using FlowJo software.

### ***Assessment of renal dysfunction***

Proteinuria and hematuria were monitored in some experiments using AlbuStix indicator sticks and read on a Clintek Status machine (Bayer) or by direct quantitative urinalysis using the Olympus Clinical Chemistry Analyzer AU400e (albumin, creatinine, total protein, and urea nitrogen). Determinations were as per manufacturer's specification for human urine, except that the albumin concentrations were multiplied by a factor of 3 to account for diminished sensitivity to mouse albumin.

### ***Histological analysis***

Formalin-fixed, paraffin embedded kidneys were sectioned (5 µm) and stained with Periodic Acid Schiff (PAS) or Masson's Trichrome and for monocytes by immunohistology with F4/80. For immunofluorescent analyses, kidneys were suspended in OCT, frozen and sectioned at 7 µm. Acetone fixed sections were stained using FITC-conjugated antibodies to IgA, IgG and IgM (Southern Biotech) and C4 (Cedarlane).

### ***Quantitative Real-Time RT-PCR***

For assessment of RNA transcript levels, tissues were homogenized and RNA isolated using Qiagen Midi Kit. DNase I treated RNA was reverse transcribed using random hexamer primers (High Capacity cDNA Archive Kit, ABI). Real-time quantitative RT-PCR was performed using the Stratagene Mx3000P system. Primers and probes were designed using Primer Express software (Applied Biosystems). The sequences used to detect total BAFF (Tnfsf13B) levels were forward primer 5'-CCATCACTCCGCAGAAGGA, reverse primer, 5'-GCCTTCCATCCCTGCAGAT, 6FAM-probe 5'-AGGGTGCCTGGTTT. Endogenous BAFF : 6FAM probe 5'-CCAAACCAGGAAATAT; forward primer 5'-TCGTGACCCGTTGAATCTGA; reverse primer 5'-ACTTCGGTTGTGGCTGTCTGT (Figure 1D). The sequences used to detect the secreted splice form of mouse IgA were: 6FAM probe, 5'-

CAGAAGACCATCGACC; forward primer 5'-GCCTTGCCCATGAACTTCAC; reverse primer, 5'-CGCTGACATTGGTGGGTTTA. All gene expression was normalized to the housekeeping gene GAPDH : 6FAM probe, 5'-CCCCAATGTGTCCGTC; forward primer 5'-CATGGCCTTCCGTGTTCCCTA; reverse primer, 5'-GCCGGCACGTCAGATCCA.

For assessment of zygosity of BAFF-Tg mice, DNA was prepared from tail biopsies (Qiagen DNeasy Blood and Tissue kit). The ratio of total BAFF to endogenous BAFF was examined using qPCR as described above with exception of the usage of a different set of primers/probe for total BAFF: 6FAM probe 5'-CAAGACTGTCTGCAGCTG; forward primer 5' - TGGAATGAACCTCAGAAACATCA; reverse primer 5'-GCGTGTCGCTGTCTGCAA.

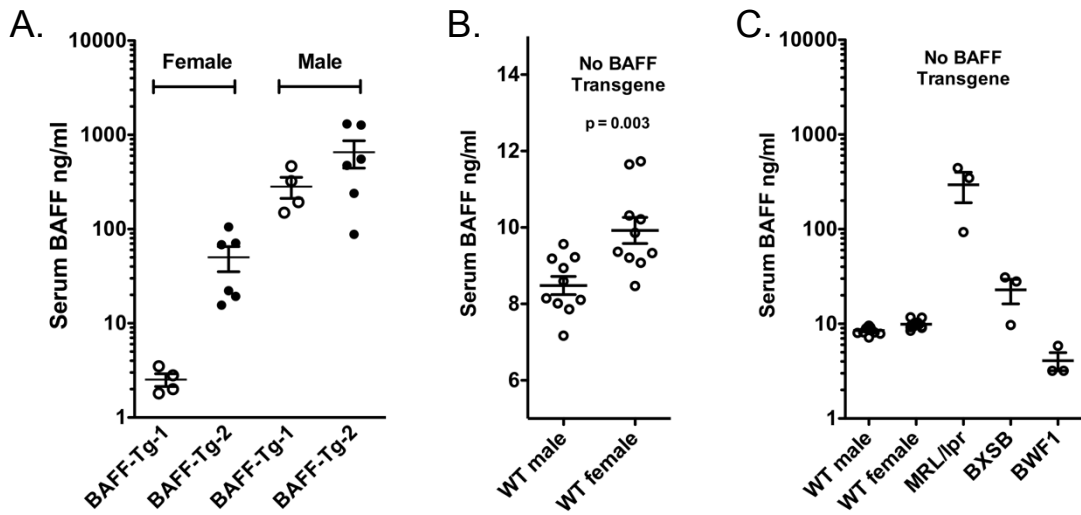
## References

1. Veniant, M., Menard, J., Bruneval, P., Morley, S., Gonzales, M.F., and Mullins, J. 1996. Vascular damage without hypertension in transgenic rats expressing prorenin exclusively in the liver. *J Clin Invest* 98:1966-1970.
2. Suzuki, K., Meek, B., Doi, Y., Muramatsu, M., Chiba, T., Honjo, T., and Fagarasan, S. 2004. Aberrant expansion of segmented filamentous bacteria in IgA-deficient gut. *Proc Natl Acad Sci U S A* 101:1981-1986.
3. Gaboriau-Routhiau, V., Rakotobe, S., Lecuyer, E., Mulder, I., Lan, A., Bridonneau, C., Rochet, V., Pisi, A., De Paepe, M., Brandi, G., et al. 2009. The key role of segmented filamentous bacteria in the coordinated maturation of gut helper T cell responses. *Immunity* 31:677-689.
4. Ivanov, II, Atarashi, K., Manel, N., Brodie, E.L., Shima, T., Karaoz, U., Wei, D., Goldfarb, K.C., Santee, C.A., Lynch, S.V., et al. 2009. Induction of intestinal Th17 cells by segmented filamentous bacteria. *Cell* 139:485-498.
5. Lee, Y.K., Menezes, J.S., Umesaki, Y., and Mazmanian, S.K. 2010. Proinflammatory T-cell responses to gut microbiota promote experimental autoimmune encephalomyelitis. *Proc Natl Acad Sci U S A* 108:4615-4622.
6. Van Snick, J.L. 1981. The production of anti-IgG2a autoantibody in the 129/Sv mouse: onset in the lymph nodes draining the intestinal tract and prevention by neonatal thymectomy. *J Immunol* 126:815-818.

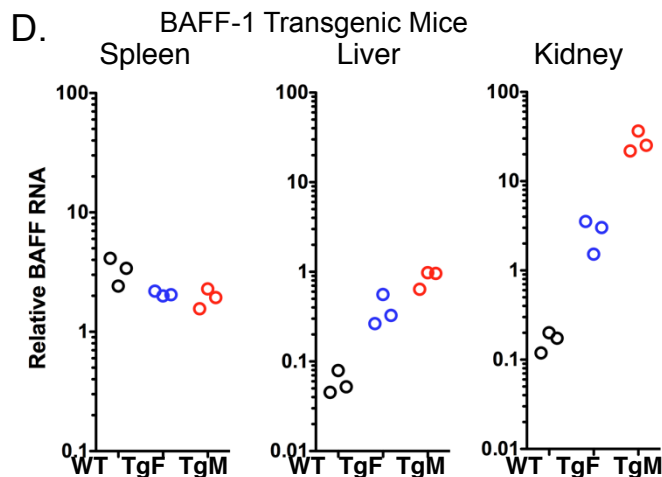
## Supplemental Figure 1:

**In BAFF-Tg mice, BAFF protein levels are preferentially elevated in male mice and the kidney is the dominant source of BAFF.**

Serum BAFF levels in various mice. A). BAFF-Tg mice at 12 weeks of age in the two lines. Male mice have more serum BAFF. B). Expanded scale showing slightly more BAFF in C57BL6 females mice (ages 3-9 Mo). Differences between WT and BAFF-1-Tg females simply reflect assays run with different ELISAs and do not represent a fundamental difference. C). For reference, a comparison to normal and diseased female MRL/lpr, (male and female) BXSB (male) and BWF1 (female) mice where diseased mice had albuminuria scores above ~300 mg/dl.

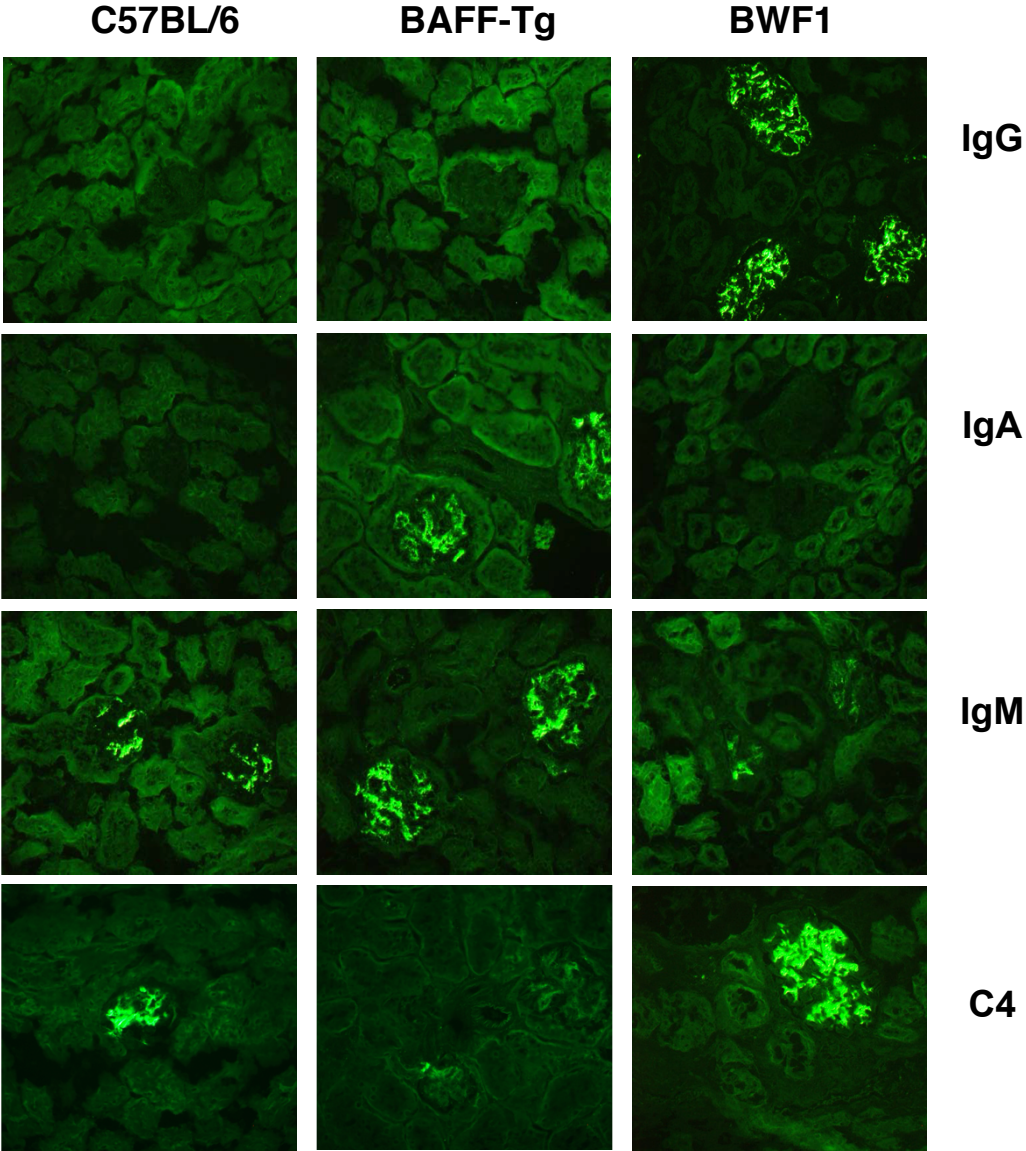


D). BAFF mRNA levels by Q-PCR in the spleen, kidney and liver of BAFF-1 Tg (representative of both Tg lines). High-level kidney expression of the BAFF transgene is found in the kidney and male mice have 10-fold higher levels in the kidneys than female mice. These primers detected both endogenous and transgenic transcripts and data are normalized to GAPDH. Both transgene and endogenous-BAFF specific primer sets were investigated separately and the kidney BAFF was transgene-derived. mRNA levels were also found to correlate with protein BAFF levels by Western blot (not shown).



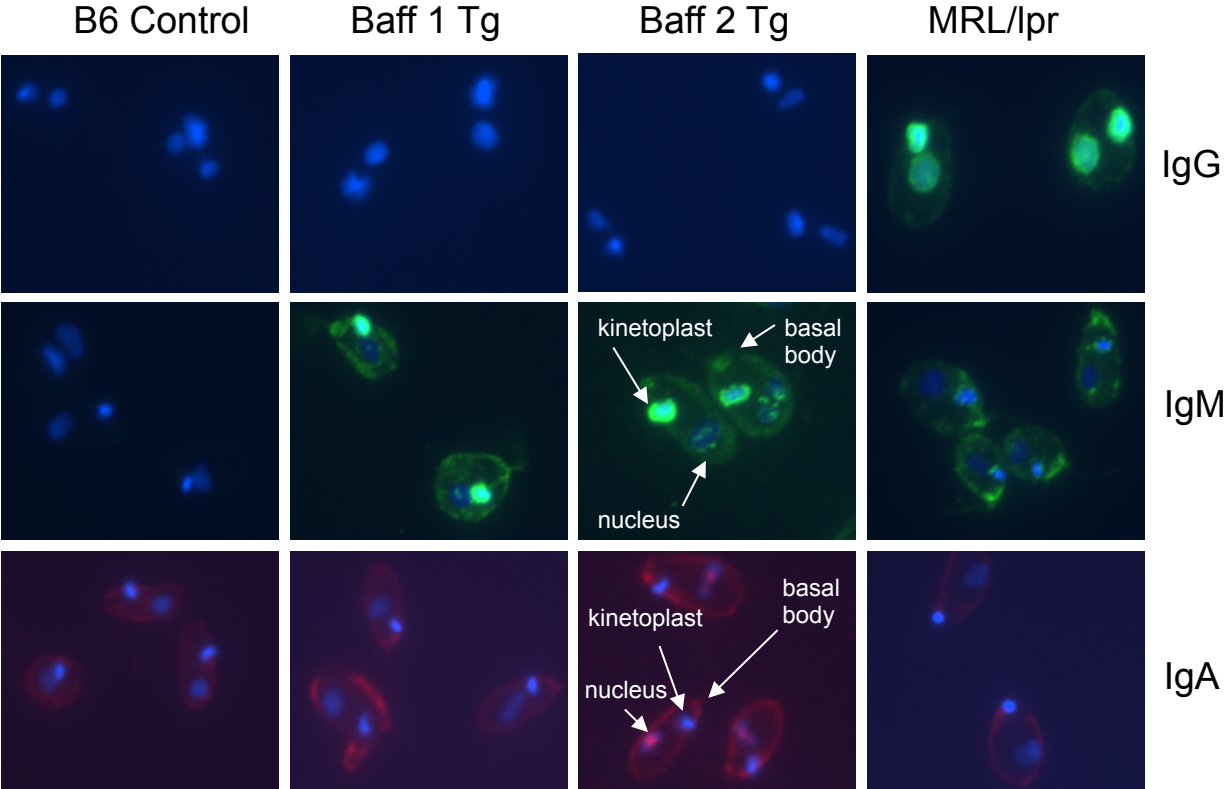
**Supplemental Figure 2:**

Comparison of IgG, IgM and IgA deposition in 8 month-old male WT, male BAFF-1-Tg and female BWF1 (NZB x NZW F1) kidneys (100X) using FITC-conjugated isotype and complement-specific antibodies. IgA staining was performed with a mixture of IgG1, IgG2a, IgG2b and IgG3 specific antibodies to ensure reactivity with all isotypes. Representative images show glomerular mesangial deposition of IgA and IgM in BAFF-Tg mice. In contrast to BWF1 glomeruli, C4 deposition was not predominant in BAFF-Tg mice.



**Supplemental Figure 3:**

Crithidia immunofluorescence assay shows the presence of only IgM anti-dsDNA (kinetoplast) in male BAFF-1 and BAFF-2 transgenic mouse serum. Staining is Hoeschst Dye DNA (blue), IgG and IgM (green) and IgA (red). Parasites were stained with serum at a 1:10 dilution.



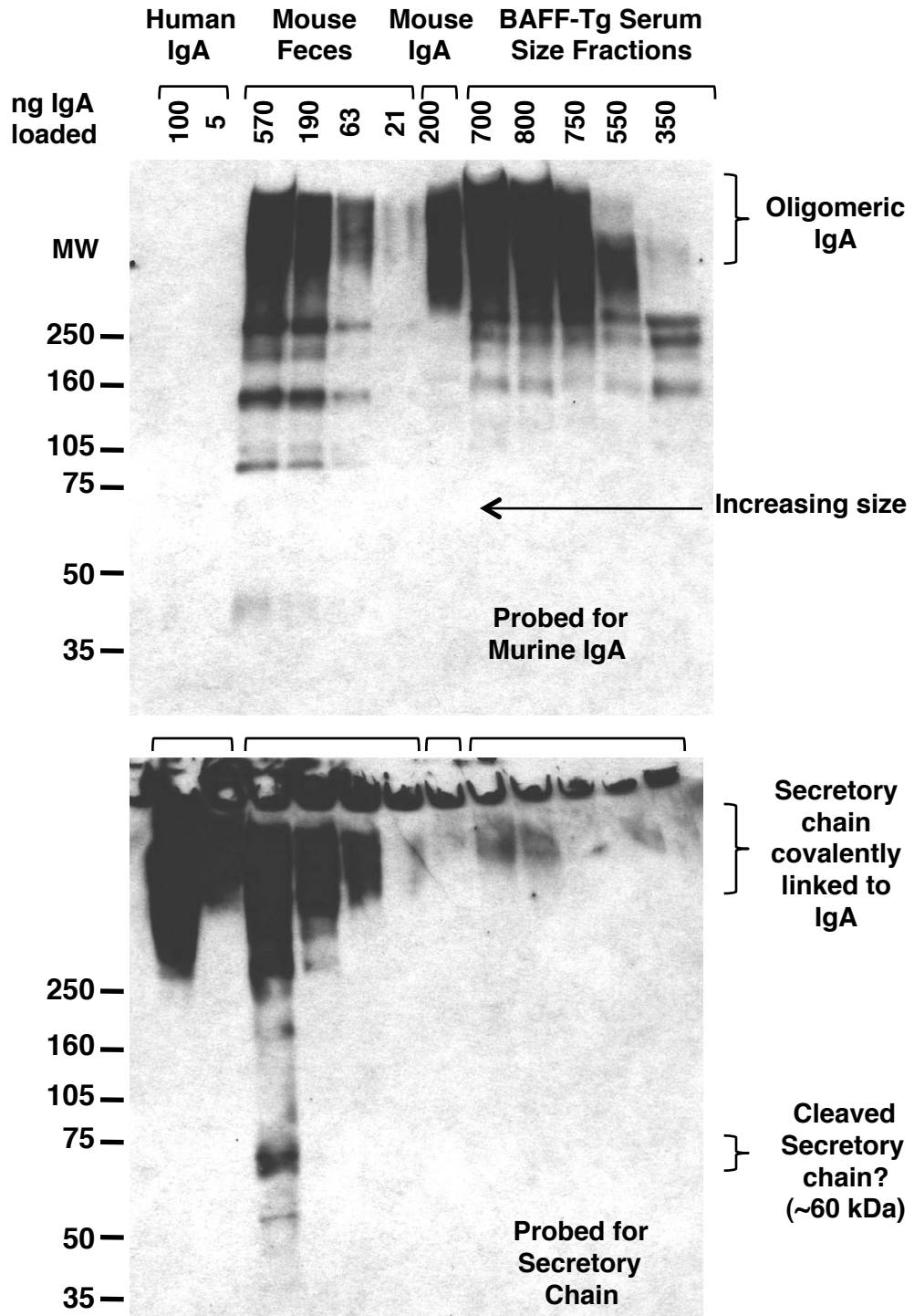
## **Supplemental Figure 4:**

### **Failure to detect secretory chain associated with polymeric IgA in the sera of BAFF-Tg mice.**

Western blot analysis of the fractions off the sizing column resolution of male BAFF-Tg serum for IgA and secretory chain. For comparison, controls include a mouse fecal sample (for murine secretory chain), myeloma-derived murine IgA (clone TEPC 15 BD Biosciences) and human colostrum derived IgA (Sigma) which contains human secretory chain. Separate blots from 2-15% acrylamide gels run under non-reducing conditions were probed with HRP-conjugated goat anti-mIgA (Southern Biotech) or rabbit anti-human secretory chain (Dako) followed by goat (Fab2) anti-rabbit IgG-HRP. Prior analysis had shown that there was sufficient cross-reactivity of the polyclonal rabbit anti-human secretory chain antibody to recognize the mouse protein. Secretory chain is covalently linked to oligomeric IgA during export and hence runs with the IgA. Despite loading up to 0.8 ug of IgA on the lane, the secretory chain was not readily detected in size-fractionated BAFF-Tg blood (only traces in fractions 10 and 12), whereas it was readily observed using 63 ng fecal IgA from BAFF-Tg mice or 5 ng of human colostrum derived IgA (IgA ELISA determinations on BAFF-Tg serum fraction or the fecal extract guided loading). As expected, secretory IgA was not detected in commercial IgA purified from a myeloma cell line. Fractions from the BAFF-Tg blood correspond to #10, 12, 14, 16 and 18 from figure 3. Preservation of high molecular weight polymeric IgA after boiling in SDS and SDS-PAGE indicates that the high molecular-weight IgA is unlikely to be the result of immune complex formation.

# Supplemental Figure 4:

## Western Analysis of Nonreduced IgA and Secretory Chain

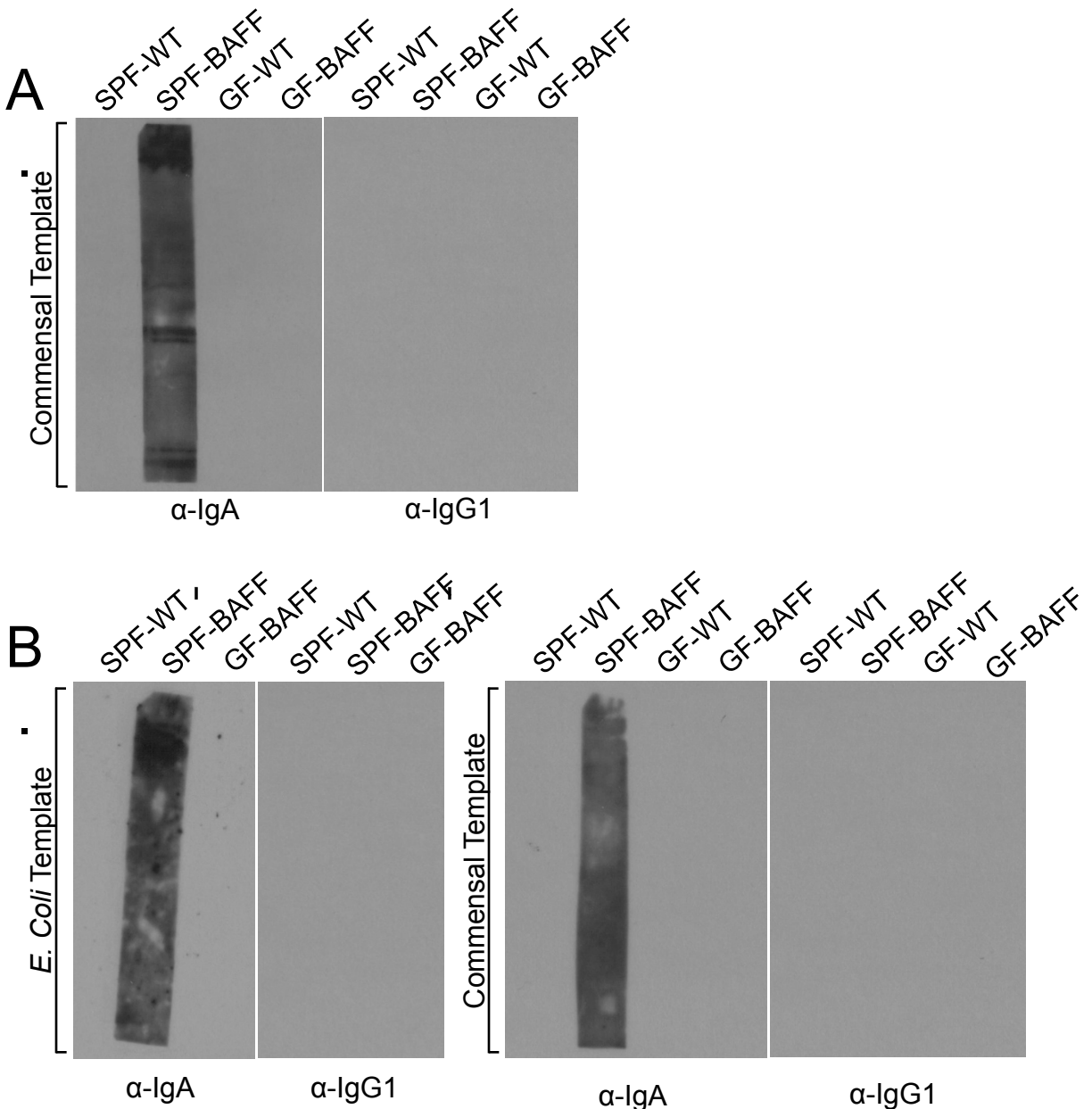




## Supplemental Figure 5:

### SPF-BAFF-Tg mice possess commensal-reactive IgA in both their serum and kidneys.

Commensal reactivity was evaluated by western blot. Serum (A) or homogenized kidney tissue (B) samples from wild type (WT) or BAFF-Tg mice housed in either specific pathogen free (SPF) or germ free (GF) facilities was diluted into blocking buffer and used as the western blot primary antibody solution. A commensal bacteria or *E. coli* template was generated as in Fig. 4., loaded onto nitrocellulose membrane and cut into strips. (A) Serum from SPF-WT, SPF-BAFF-Tg, GF-WT and GF-BAFF-Tg mice was diluted 1/500. Only SPF-BAFF-Tg serum displayed commensal reactivity. A secondary IgG1 probe was used on a duplicate set of membranes with no reactivity. (B) Homogenized kidney eluate from the same groups above was loaded onto nitrocellulose membrane strips containing an *E. coli* (left) or a commensal template (right). Similar to (A), only SPF-BAFF-Tg kidney solution showed reactivity. A secondary IgG1 probe was again used on a duplicate set of membranes with no reactivity.



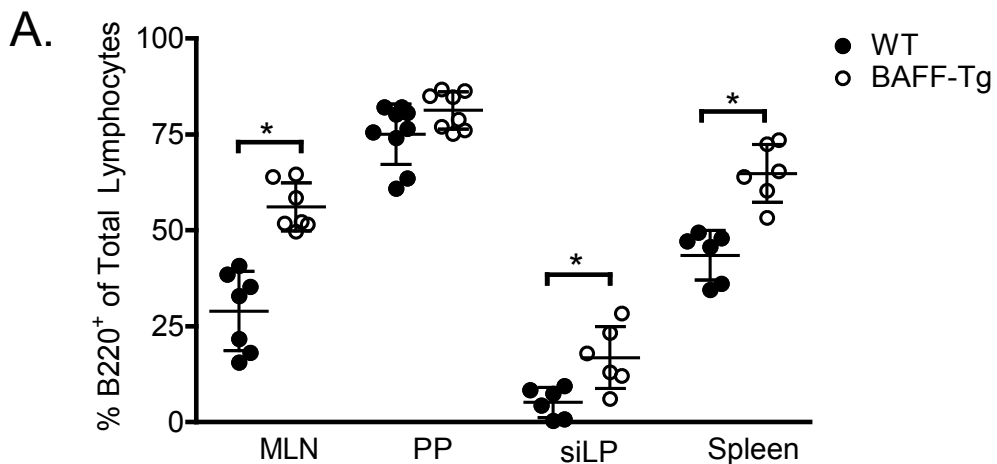
## Supplemental Figure 6:

### **B cell hyperplasia in mucosal and peripheral tissues accompanied by increased IgA plasma cells throughout the periphery is observed in BAFF-Tg mice.**

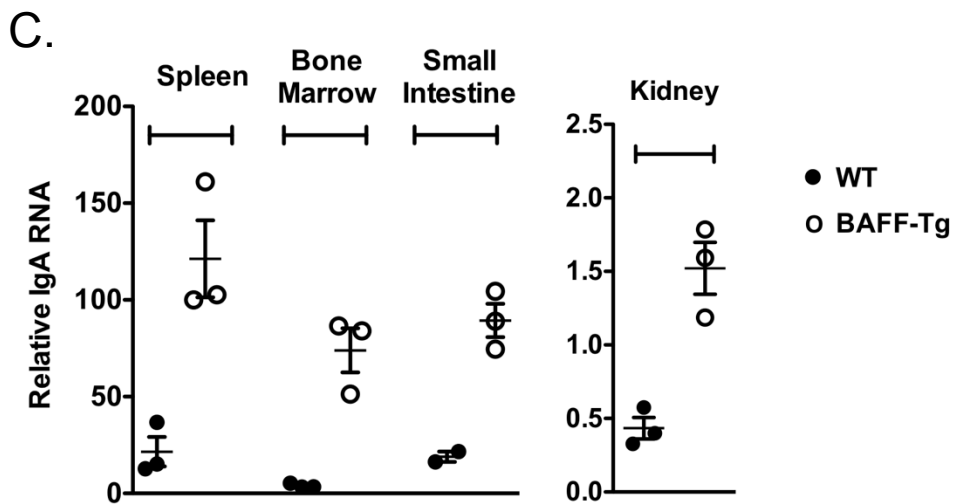
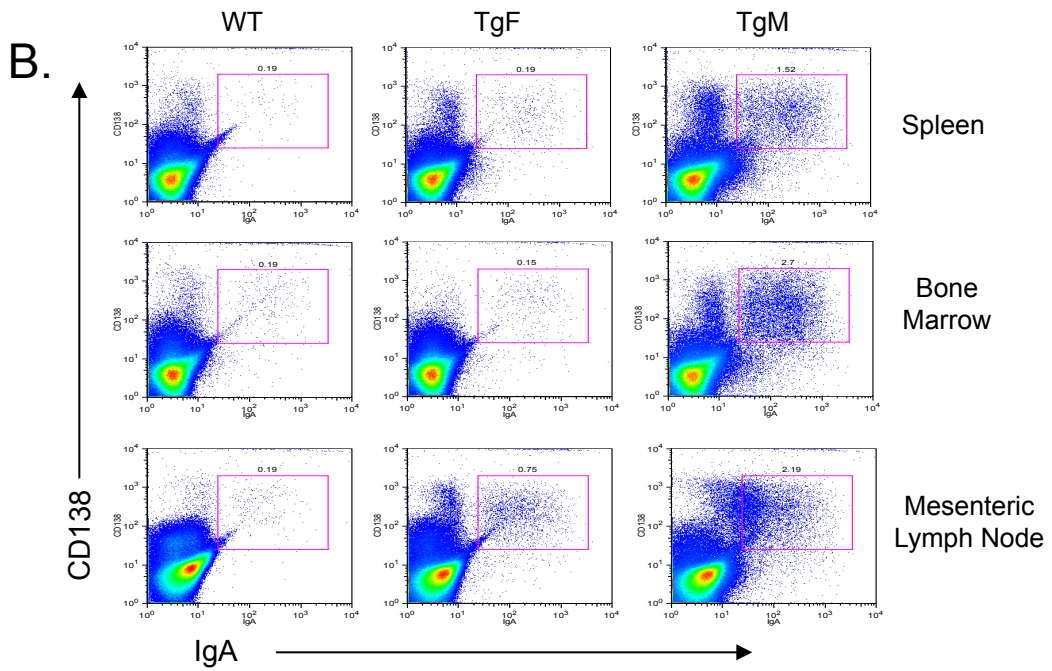
A). Quantification of B220+ CD19+ B cells in mucosal tissues and spleen of 12 week-old C57BL/6 or BAFF-2 transgenic mice. B cell compartment size is increased in the LP of the small intestine (siLP) and as expected the B cell compartment size is increased in mLN and spleen with less of an increase in the Peyer's patch (PP).

B). FACS analysis of spleen, BM and mLN from 4 month-old homozygous BAFF-Tg-2 mice reveals an increase in CD138+, intracellular IgA+ plasma cells.

C). Quantitative PCR using reagents specific for the secretory IgA splice form (sIgA) was used to determine the relative levels of sIgA in RNA isolated from spleen, bone marrow, small intestine and kidney of wild-type, and BAFF-Tg (Homozygous BAFF-Tg-1 males, 3mo) mice. sIgA levels are normalized to GAPDH to give the relative expression values. Open circle, BAFF-Tg; solid circles, WT (C57BL/6 Charles River)



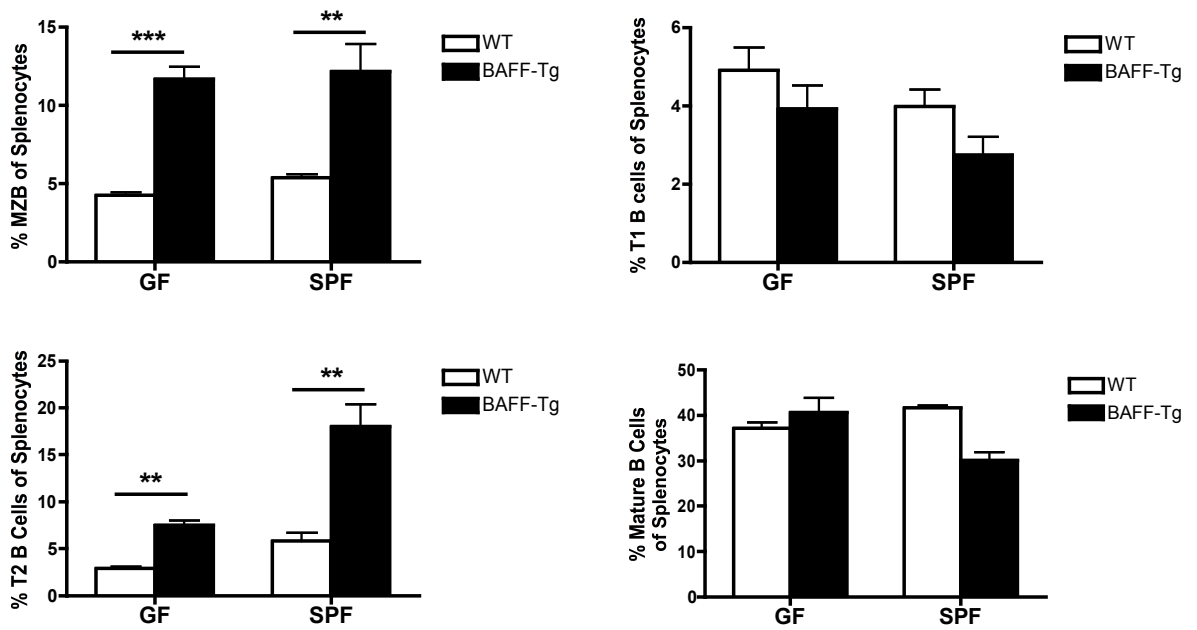
Supplemental Figure 6 Cont' :



## Supplemental Figure 7:

### BAFF-driven expansion of splenic marginal zone and transitional Type 2 B cell subsets occurs normally in germ-free BAFF-Tg.

Lymphocytes from C57Bl/6 and age-matched BAFF-2 transgenic Tg GF and SPF mice were analysed by flow cytometry to determine frequency of specific B cell subsets as a percentage of total lymphocytes in the spleen.



## Supplemental Figure 8:

### BAFF-Tg Kidney Pathology is altered in the absence of IgA

A). Analysis of BAFF1 x IgA<sup>+/+</sup> mice at varying ages showing elevated serum IgA and the drop with age presumably due to loss of BAFF transgene expression (not shown). BAFF parent refers to homozygous BAFF1-Tg mice without crossing to the IgA deficiency. Assay limits in this format were around 10-60 ug/ml. IgA deficient mice lacked detectable IgA.

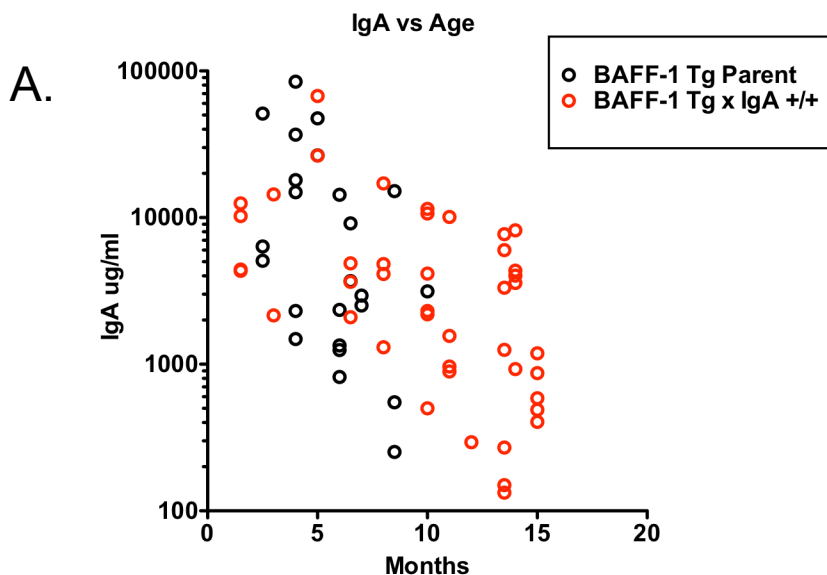
B-E). Images of kidneys from BAFF1 Tg mice on IgA<sup>+/+</sup> and IgA<sup>-/-</sup> backgrounds at 14 to 15 months.

B) Analysis of Ig deposition in the kidneys of BAFF-1 x IgA<sup>-/-</sup> mice using polyclonal anti-IgA and IgG reagents (goat anti-mouse IgA and Ig $\gamma$  chain, Southern Biotech 1045-02, 1030-02) that were optimally titrated using kidneys from diseased BWF1 (7 weeks after receiving adenoviral-IFN $\alpha$  to accelerate disease) and aged C57Bl/6 mice (as positive and negative standards). As older B6 mice often have positive glomeruli, the optimal Ab titering led to the relatively weak staining shown for BWF1. Two examples of a BAFF-1 x IgA<sup>+/+</sup> mouse showing the variable levels IgA complexes at 14-15 months as well as the IgG deposition often observed at this stage. Two examples of BAFF-Tg x IgA<sup>-/-</sup> mice showing similar IgG deposition, but no IgA. Labels state the albuminuria (PU, dipstick) scores and serum IgA levels.

C). Masson's-Trichrome stain showing reduced glomerular matrix deposition in the absence of IgA. These mice had similar proteinuria scores (greater than 100 mg/dl) at harvest. As staining was performed in different runs, the color was adjusted in Photoshop to normalize the tubular epithelial staining.

D) Examples of reduced glomerular nephritis with fewer F4/80-positive monocytes surrounding the capsule in BAFF-1 x IgA<sup>-/-</sup> mice. Tubulointerstitial monocytes were present in kidneys from BAFF-1 Tg mice with proteinuria regardless of IgA status. The numbers of interstitial monocytes were not elevated in non-transgenic IgA<sup>-/-</sup> mice and there was no discernable difference between non-transgenic IgA<sup>+/+</sup> and IgA<sup>-/-</sup> mice. Both mice exhibited mild proteinuria (trace to +) at this stage.

E). Higher magnification view of the type of staining shown in D but showing different regions. Intra-glomerular F4/80-positive monocytes were not observed in sick BAFF-Tg IgA<sup>+/+</sup> mice; however, they were frequently observed in transgenic IgA<sup>-/-</sup> mice that had proteinuria. Block arrows point to peri-glomerular clusters and arrowheads indicate intra-glomerular monocytes.



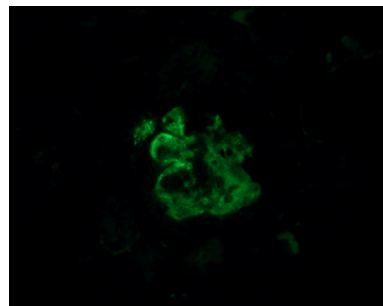
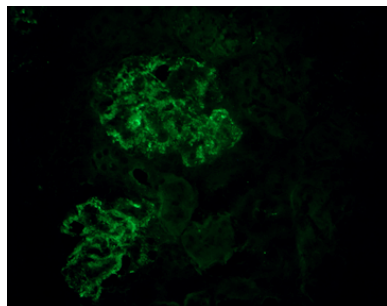
# Supplemental Figure 8 Continued

B.

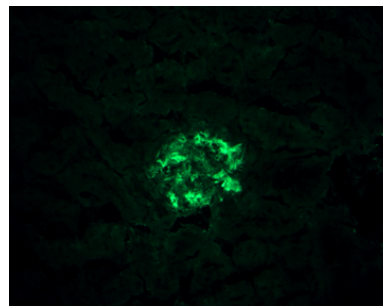
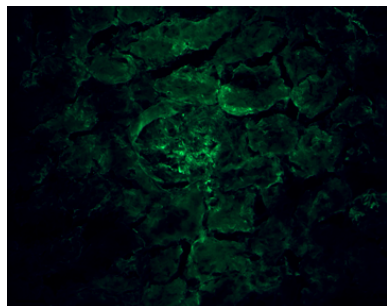
IgG

IgA

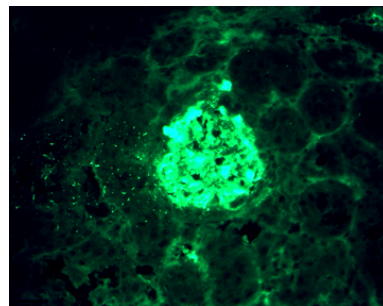
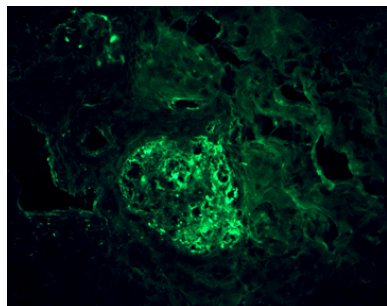
BWF1  
Adeno-IFN  
7 weeks



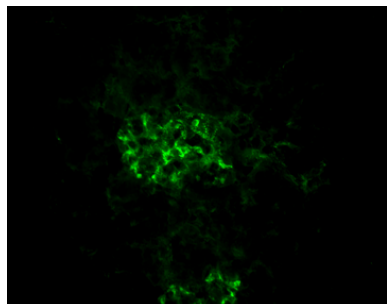
BAFF-Tg x IgA+/+  
15 Mo PU +  
IgA 489 µg/ml



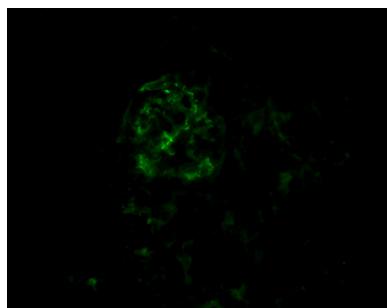
BAFF-Tg x IgA+/+  
14 Mo PU ++  
IgA 4352 µg/ml



BAFF-Tg x IgA-/-  
14.5 Mo PU trace



BAFF-Tg x IgA-/-  
13.5 Mo PU +++





## Supplemental Figure 8 Continued

